Liquid acrylate-endcapped biodegradable poly(ε-caprolactone-*co*-trimethylene carbonate). II. Computer-aided stereolithographic microarchitectural surface photoconstructs

Takehisa Matsuda,[1] Manabu Mizutani[2]
[1]*Department of Biomedical Engineering, Graduate School of Medicine, Kyushu University, 3-1-1 Maidashi, Higashi-ku, Fukuoka 812-8582, Japan*
[2]*Department of Bioengineering, National Cardiovascular Center Research Institute, 5-7-1 Fujishiro-dai, Suita, Osaka 565-8565, Japan*

Received 29 November 2001; revised 14 February 2002; accepted 14 February 2002

Abstract: Advanced micromedical devices may require computer-aided photofabrication, by which microarchitectural surface design and entire macroshaped body design are feasible. Liquid acrylate-endcapped poly(ε-caprolactone-*co*-trimethylene carbonate)s, poly(CL/TMC)s, prepared using trimethylene glycol (TMG) or poly(ethylene glycol) (PEG) as an initiator and an acrylate group for subsequent terminal capping, were used as photocurable copolymers. The stereolithographically microarchitectured photoconstructs were prepared using a custom-designed apparatus with a moving ultraviolet (UV) light pen driven by a computer-assisted design program. The prepared photoconstructs included microneedles, a microcylinder and microbanks on surfaces. *In vitro* hydrolytic degradation proceeded with surface erosion when hydrophobic TMG-based photocured copolymers were employed, whereas very fast degradation of hydrophilic PEG-based photocured copolymers probably via concerted actions of surface erosion and bulk degradation was observed. *In vivo* hydrolytic behavior upon subcutaneous implantation in rats indicated that surface erosion proceeded for TMG-based photoconstructs. Anti-inflammatory drug (indomethacin) loading into microneedle-structured surfaces minimized inflammatory reactions. The possible biomedical microarchitectural three dimensinal in biomedical application photoconstructs was discussed. © 2002 Wiley Periodicals, Inc. J Biomed Mater Res 62: 395–403, 2002

Key words: photocuring; stereolithography; biodegradable; surface erosion; drug immobilization

INTRODUCTION

Photofabrication of microdevices and microarchitectured surfaces may be required for advanced medical procedures.[1–4] To this end, the authors have been developing photocurable biodegradable liquid copolymers and its photofabrication process. Photocurable liquid copolymers designed and develop to this end were composed of trimethylene carbonate (TMC) and ε-caprolactone (CL), and were di-, tri-, and tetra-branched, each termini of which was capped with a coumarin,[5–8] phenylazide,[9] or acrylate group.[10] When low molecular-weight alkane diol, triol, or tetraol as an initiator was utilized, hydrophobic, water nonabsorbable photocured copolymers were obtained. On the other hand, when poly(ethylene glycol) (PEG) and its tetra-branched derivative were used as an initiator, hydrophilic, water-adsorbable photocured copolymers were obtained.

In this article, as an extension of our series of studies, microarchitectural surfaces were prepared using bifunctionally acrylate-endcapped hydrophobic and hydrophilic copolymers composed of TMC and CL at an equimolar basis. Figure 1 shows the structure of photopolymerizable copolymers used (**a** and **b**). Using a custom-designed stereolithographic rapid prototyp-

Correspondence to: T. Matsuda; e-mail: matsuda@med.kyushu-u.ac.jp
Contract grant sponsor: Johnson & Johnson Medical Japan, Tokyo, Japan (to M.M.)
Contract grant sponsor: The Promotion of Fundamental Studies in Health Science of the Organization (for Pharmaceutical Safety and Research—OPSR); contract grant number: 97-15

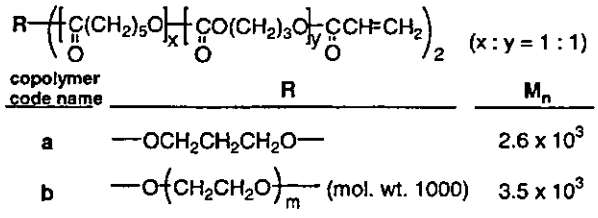

Figure 1. Structure and molecular description of bifunctional acrylate-endcapped poly(CL/TMC)s.

ing apparatus (SLA) with ultraviolet (UV) light, microarchitectured surfaces were prepared. *In vitro* and *in vivo* hydrolysis behaviors of photoconstructs and drug loading and *in vivo* release from upon implantation of photoconstructs into subcutaneous tissues were demonstrated.

EXPERIMENTAL

General procedure

All of the solvent and reagents were purchased from Wako Pure Chemical Industries, Ltd. (Osaka, Japan) or Sigma-Aldrich Japan, Inc. (Tokyo, Japan). Trimethylene carbonate (TMC) was prepared according to the method previously reported, and recrystallized from a mixed solvent of ethyl acetate and hexane.[5] Other solvents and reagents were purified by distillation. ^{1}H-NMR spectra were recorded on a JEOL JNM-GX270 FT-NMR spectrometer (270 MHz, Tokyo, Japan). The chemical shifts were given as δ values with Me_4Si as the internal standard. Ultraviolet (UV) absorption spectra were measured on a JASCO Ubest-30 UV/VIS spectrometer (Tokyo, Japan). UV irradiation was carried out using a 250 W mercury-xenon (Hg-Xe) lamp (Hamamatsu Photonics L5662-02, Shizuoka, Japan). The intensity of UV light was measured at 250 nm on a TOPCON UVR-25 (Tokyo, Japan). The surface topographic changes of were determined by scanning electron microscopy (SEM; JEOL JSM-6301F, Tokyo, Japan). The histological observation of subcutaneous tissues of rats was carried out by light microscopy (Olympus VANOX-S AHBS, Tokyo, Japan).

Synthesis of acrylate-endcapped poly(ε-caprolactone-*co*-trimethylene carbonate) copolymer, acrylated poly(CL/TMC)

The preparation of acrylated poly(CL/TMC) was carried by a two-step reaction. First, poly(CL/TMC)s were prepared using CL and TMC as (co)monomers, trimethylene glycol or poly(ethylene glycol) (PEG, mol. wt. 1000) as an initiator and tin(II)2 ethylhexanoate as a catalyst at almost full conversion.[10–16] Subsequently, hydroxyl groups at terminal ends of copolymers were esterified using acryloyl chloride.[10] The compositions of the copolymers were determined by ^{1}H-NMR spectroscopy, and the acrylate content and molecular weight of the acrylate-endcapped copolymer were determined from the relative peak intensities between the acrylate group of the copolymer and methylene groups ascribed to the coumarin group of the coumarin-endcapped copolymer used as a reference compound at the same concentration in ^{1}H-NMR spectra (the coumarin content of the coumarinated copolymer was quantitatively determined by UV spectroscopy in our previous article[5]).

UV-induced photocuring characteristic

A round liquid film (diameter 15 mm) of the acrylate-endcapped copolymer or the mixture of the copolymer and benzophenone, which was coated on a coverglass, was irradiated using a Hg-Xe lamp at 10 mW/cm^2. After immersion in dichloromethane to dissolve the solvent-soluble part, the insoluble copolymer was dried and weighed. The photocuring yield was defined as the weight percentage of the insoluble part (W_g) relative to that of the coated copolymer (W): $W_g/W \times 100$.

Water adsorptivity

A round photocured film was immersed in water for two days at room temperature. The degree of water adsorptivity (DW) was determined as the relative amount of water uptake relative to that of the dried photocured copolymer on the basis of weight.

Photofabrication using a stereolithographic apparatus (SLA)

Photofabrication of microarchitectural blocks using a custom-designed SLA was carried out as follows (Fig. 2). The SLA consisted of a moving light pen with a photomask (diameter, 100 μm), an optical fiber connecting the light pen and the light source (Hg-Xe lamp), a vertical elevator and controller (Sigma Koki MARK-41, Tokyo, Japan) driven by computer-assisted design, and a liquid-polymer bath. The stage controller manipulated the movement of the light pen at a rate of 7 μm/s and photoirradiation intensity was set

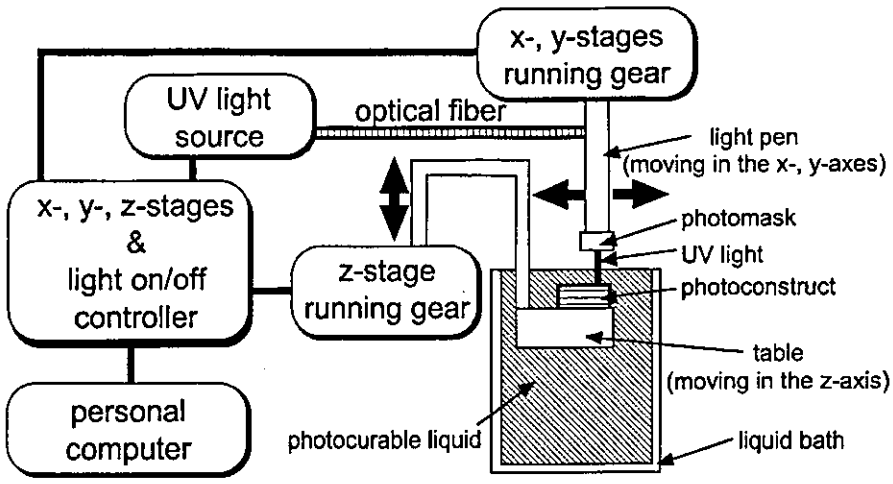

Figure 2. Schematic diagram of the stereolithographic apparatus (SLA) used.

at 50 mW/cm^2, and the liquid photoreactive copolymer was refilled on the surface by lowering the vertical elevator table into the liquid-polymer bath (200 μm/cycle), as shown in Figure 3.

Preparation of rose bengal-stained photoconstructs

Rose bengal-stained photoconstucts were obtained by immersion or partial immersion in rose bengal-saturated acetone solution for a predetermined period, washing with ethanol and air drying. The stained photoconstructs were sliced for visual cross-sectional observation.

Preparation of drug-immobilized photoconstructs

Two types of drug-immobilized photoconstructs were prepared. One was a drug-soaked construct, which was obtained by immersion of the photoconstructs in 10 wt % indomethacin-containing acetone solution for 30 min, washing with ethanol and air drying; the other was drug-capsulation construct, which was obtained by injection of 10 wt % indomethacin poly(CL/TMC) solution into a cavity of the cylindrical construct and sealing with a photocurable copolymer.

In vitro hydrolytic degradation

The photoconstruct, prepared above, was immersed in 0.1 *N* aqueous sodium hydroxide solution (pH 13). After 3 days of immersion, the photoconstruct was washed with ethanol and dried.

In vivo implantation

The photoconstructs, prepared above and washed with ethanol and air dried, were implanted under the

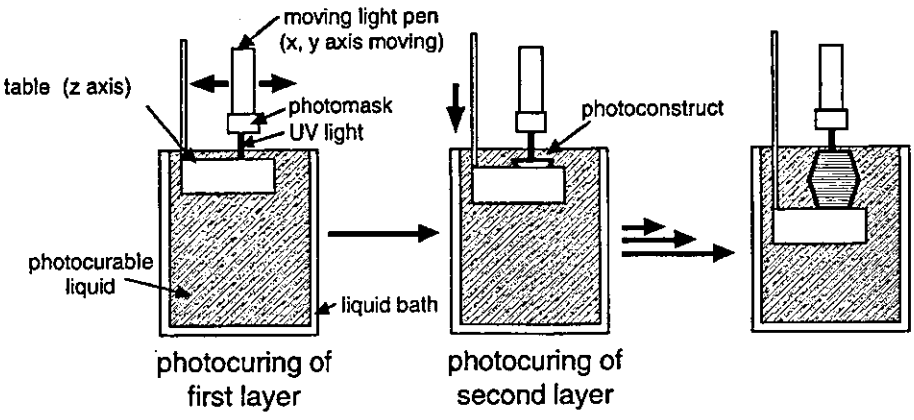

Figure 3. Layer-by-layer photofabrication in the reaction both of SLA system.

dorsal skin of male wister rats (around 400 g in weight). After a predetermined time, the rats were dissected to remove the photoconstructs from the surrounding tissues. The surrounding tissues were fixed in 1% aqueous formaldehyde solution (pH 7.4) for 12 h, and stained using hematoxylin eosin (HE) or periodic acid schiff (PAS) reaction.

RESULTS

Photocuring characteristics

Table I lists the descriptions of bifunctional acrylate-endcapped copolymers prepared using trimethylene glycol (TMG) or poly(ethylene glycol) (PEG; mol. wt. 1000 g/mol), with molecular weights of approximately 2600–3500 g/mol. The former photocured copolymer adsorbed only 1% water, whereas the latter adsorbed water of approximately one-third of its dry weight. When UV light is irradiated on a liquid film of a copolymer in the presence or absence of benzophenone as an UV-sensitive radical initiator, the photocuring yield, which is insoluble parts produced by the photoirradiation, increased with irradiation time (Fig. 4). A higher photocuring rate in the presence of benzophenone was observed for copolymer (a) compared with that in the absence of benzophenone, whereas there was little difference in the photocuring rate of copolymer (b), regardless of the presence or absence of benzophenone.

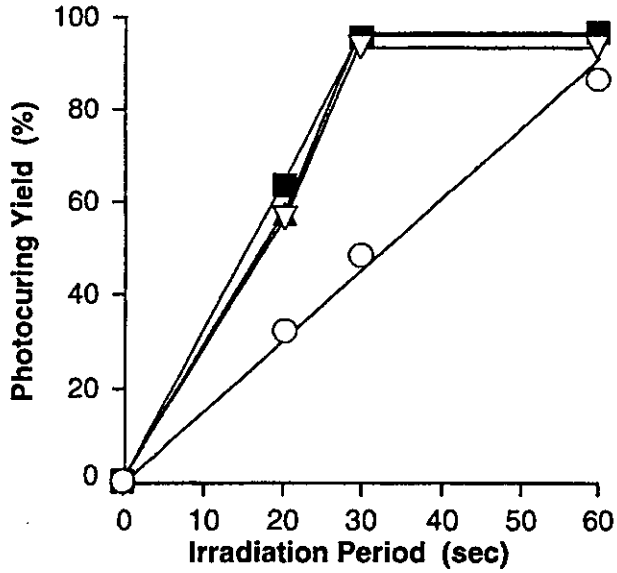

Figure 4. UV-induced photocuring characteristics of liquid films composed of diacrylated poly(CL/TMC)s at an irradiation of 10 mW/cm^2. Film thickness: 0.2 mm. Copolymer (a): ○, no initiator, ▲, 1 wt % benzophenone. Copolymer (b): ■, no initiator; ▽, 1 wt % benzophenone.

Stereolithographically prepared surfaces

A custom-designed SLA, as shown in Figure 2, which consisted of the moving light pen with the photomask with a round pore of 100 μm diameter, was operated at a moving rate of 7 μm/s. The photofabrication procedures were as follows, as shown in Figure 3. First, the stage was immersed into photocurable liquid at a depth of 200 μm, and then UV light was horizontally scanned at each 100 μm apart. The procedure was repeated two cycles to attain the flat platform's height of approximately 400 μm. Figure 5 shows design configuration of four different microstructured photoconstructs (microneedles, microcylinder, microbanks, and microwells). Figure 6 shows two examples of designed microarchitectures; microbanks, and microwells. A cylindrical photoconstruct with an inner diameter of 2.0 mm, a width of 0.2 mm, and a height of 5.0 mm was obtained by photoirradiation using the moving pen with a diameter of 2.1 mm (number of cycles: 25 cycles). Figure 7 shows the cylindrical photoconstruct thus obtained. As for the multiple microneedle architecture, the moving pen was

TABLE I
Difunctional Acrylate-Endcapped Liquid Poly (CL/TMC)

		Nonendcapped Copolymer		Acrylate-Endcapped Copolymer		
Polymer	Initiator[a]	Composition CL : TMC[b]	M_w^c	Acrylate Content[d] (mol/g)	M_w^e	DW[f]
a	$CH_2(CH_2OH)_2$	0.50 : 0.50	2200	8.1×10^{-4}	2.6×10^3	0.01
b	PEG1000	0.52 : 0.48	3300	5.7×10^{-4}	3.5×10^3	0.32

[a]Molar fraction of monomer per total OH groups of initiator was fixed at 6.6.
[b]Copolymer composition of CL/TMC determined by ^{1}H-NMR spectroscopy.
[c]Number-average molecular weight determined by GPC (PEO standard).
[d]Acrylate content determined by using the corresponding reference copolymers.
[e]Molecular weight determined based on acrylate content.
[f]Degree of water adsorption of photocured film (relative weight of water uptake to polymer).

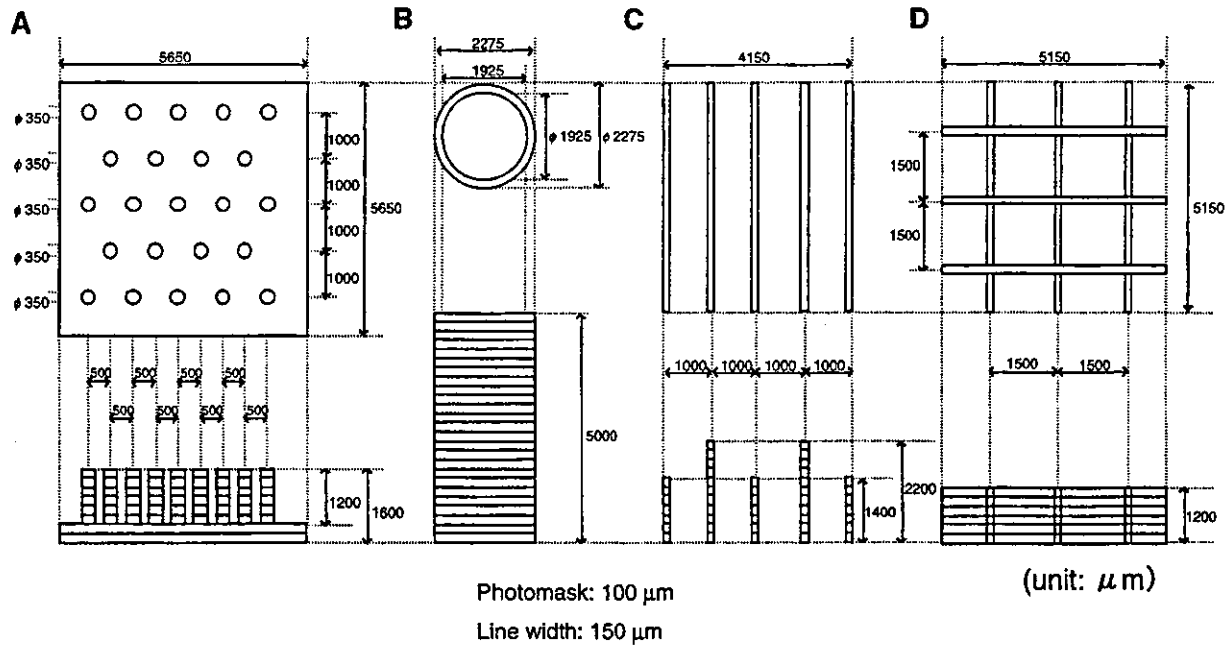

Figure 5. Design configurations of four different microstructured photoconstructs. Upper panels: top views; lower panels: cross-sectional views. (A) Microneedles; (B) microcylinder; (C) microbanks; and (D) microwells.

rotated at a predetermined location. After one spot was photocured, the light pen was moved to the next spot, which was also photocured. This sequence was repeated. After each spot was photocured, the stage was discented at a depth of 200 μm, resulting in the formation of a liquid film on the photofabricated surface. Then, such an SLA procedure was repeated again. After six cycles of the procedure were con-

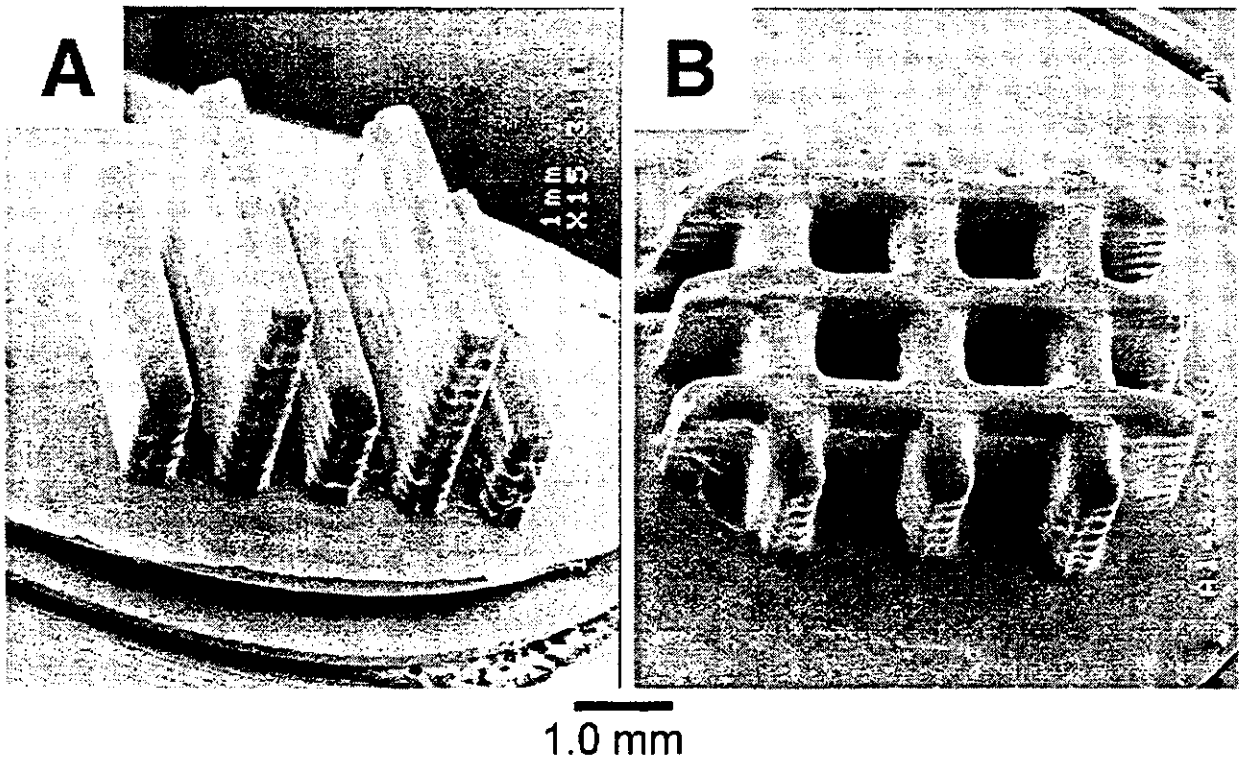

Figure 6. SEM micrographs of photoconstructs prepared from the copolymer (a). (A) microbanks; (B) microwells.

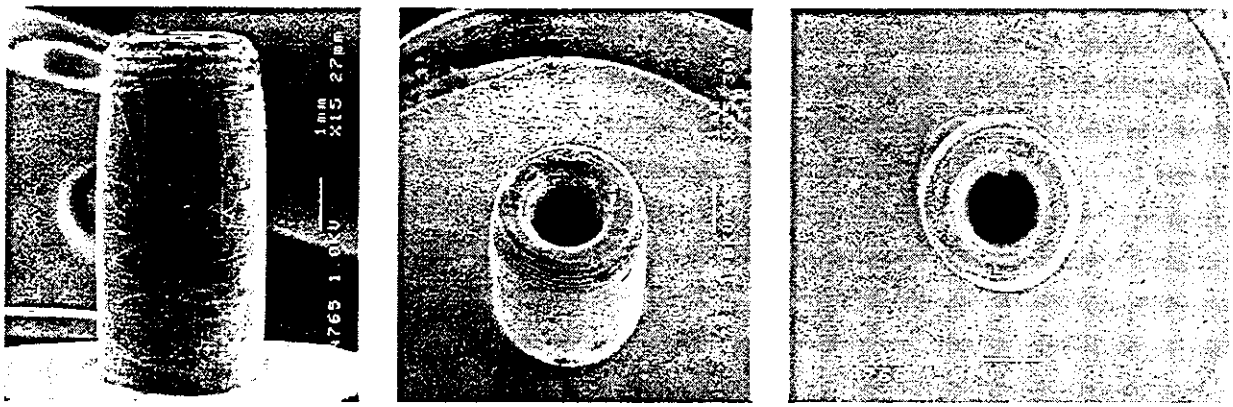

Figure 7. SEM micrographs of microcylindrical photoconstruct (left; side view, right; top view).

ducted, the surface was thoroughly washed with ethanol. The resulting microneedle-array is shown in Figure 8.

In vitro and *in vivo* hydrolysis of microneedle-like structure

The microneedle-like structured surface, which was photofabricated based on copolymer (**a**), was immersed in an alkaline solution (pH 13) for 3 days. Figure 9 shows the SEM micrographs before and after hydrolytically degraded microneedle-like structure. Upon alkaline hydrolysis, the surface became rough and the diameter became considerably smaller [approximately 70% of the original diameter; Fig. 9(B)] but the height appeared to become slightly low. This is due to the surface erosion of entire body of photoconstruct including the base platform, resulting in a very small change in the height of microneedles particularly at an early phase of hydrolysis. On the other hand, a microneedle-like photoconstruct based on PEG-based copolymer (**b**) was dissolved away within one day of immersion (data not shown).

Upon subcutaneous implantation of microneedles into a rat for 1 month, some microneedles were broken probably due to tissue movement during implantation, and the surface became rough and the diameter

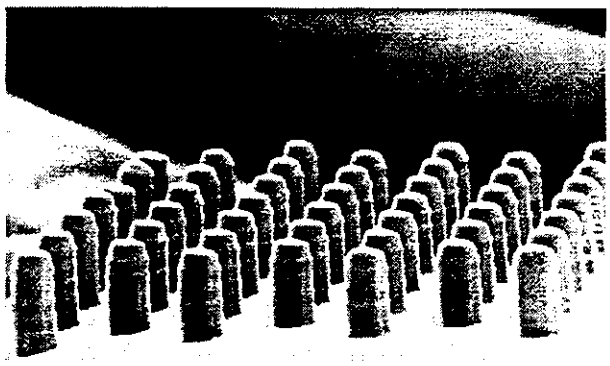

Figure 8. SEM micrographs of microneedle-array prepared from the copolymer (**a**).

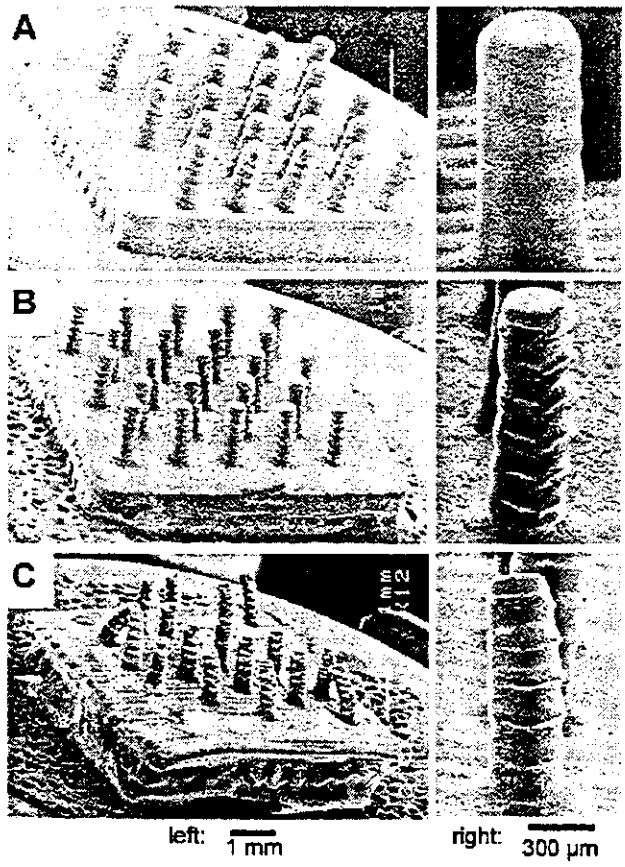

Figure 9. SEM micrographs of microneedle-like photoconstructs composed of copolymer (**a**) before and after surface erosion in alkaline solution and subcutaneous implantation. (A) Before treatment; (B) after 3 days of immersion in 0.1 *N* aqueous sodium hydroxide solution (pH 13); (C) after 1-month implantation under dorsal skin of a rat.

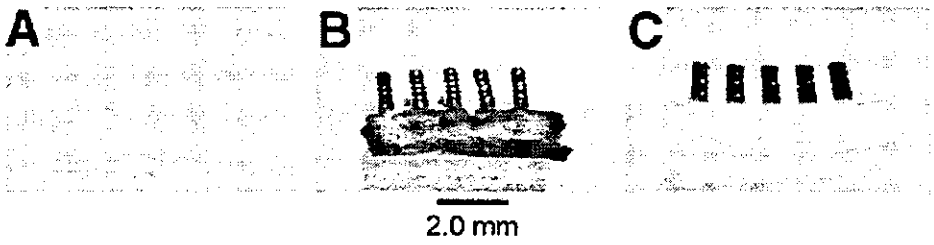

Figure 10. Cross-sectional images of sliced photoconstruct of microneedles. (A) Before immersion; (B) entire immersion in rose bengal acetone solution for 30 min; (C) partial immersion in rose bengal-containing acetone solution for 30 min.

became smaller [approximately 80% of the original diameter; Fig. 9(C)], which quite resembled with that subjected to *in vitro* alkaline hydrosis. For PEG-based copolymer (**b**), only small pieces of biodegraded photoconstructs were left in the tissues.

Drug loading on microarchitectured surface

Different procedures of drug loading on and releasing from microbanks- or microtube-structured surfaces were attempted as follows. One method was photofabrication using a liquid copolymer dispersed or dissolved with a drug. Indomethacin, which is well known as an antiflammatory drug, was selected for this purpose. However, due to the strong absorption characteristic of indomethacin (very high absorption at 300–400 nm) in UV wavelength, the drug-immobilized liquid could not be fully photocured. Alternatively, the drug was soaked after partial or full immersion of microneedle-like architectured photoconstructs in an indomethacin-containing acetone so-

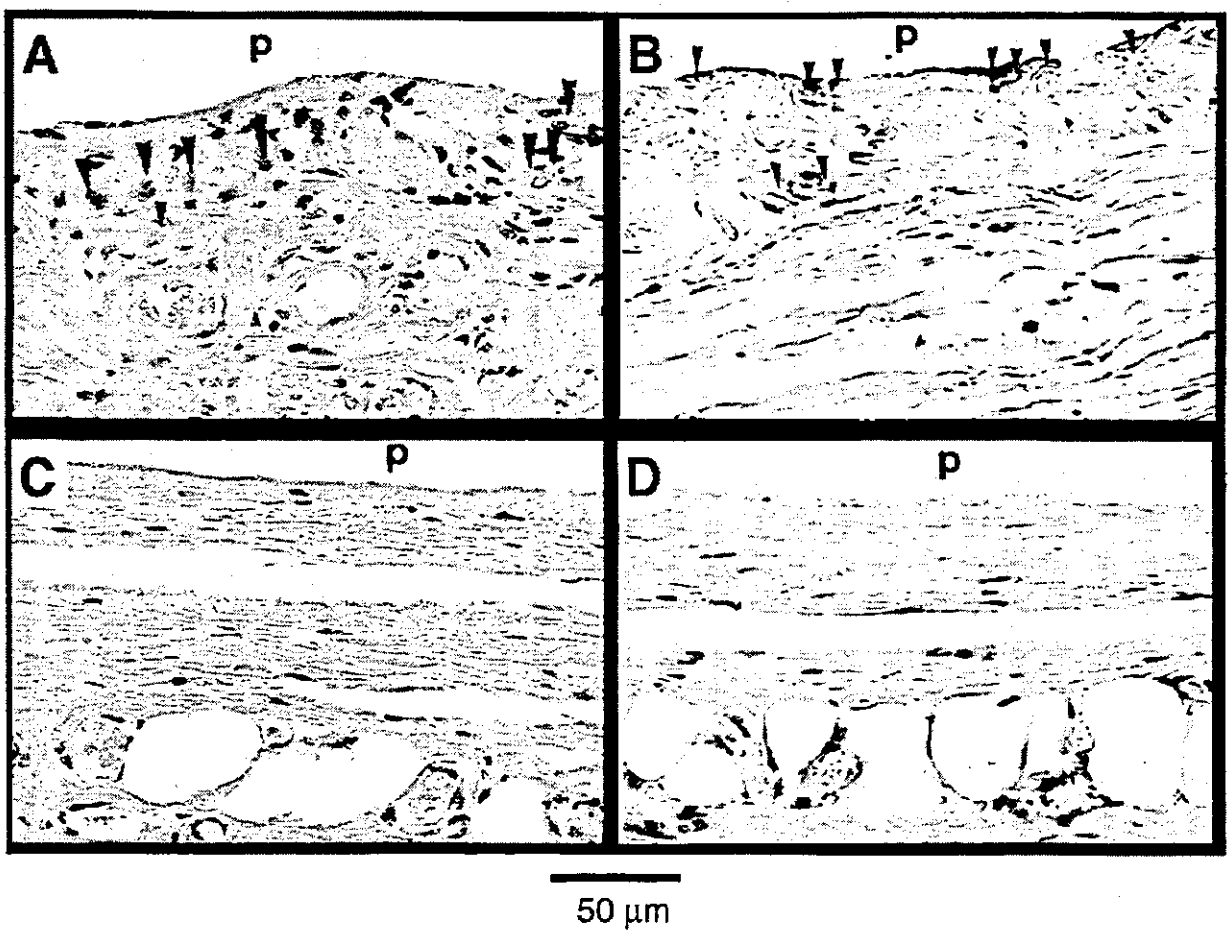

Figure 11. Histological cross-sectional photos of microfabricated photoconstruct facing subcutaneous tissues after 1-week implantation. (A, B), nonloaded; (C, D), indomethacin-loaded. (A, C) HE-stained; (B, D) PAS-stained. **p**: The space occupied by the photocured film (note that photoconstruct film became very slippery due to surface hydrolysis and was spontaneously detached at the time of retrieval). Arrows: multinucleated-like cell.

lution. To visualize the state of drug immobilization, a red-colored dye, rose bengal, was employed as a test substance. Figure 10 shows cross-sectional views of the rose bengal-stained, sliced microtectured surfaces [Fig. 10(A)]: one micrograph shows partial staining, in which dye soaking is limited to microneedle-like structural regions when only microarchitectural parts were soaked [Fig. 10(C)], and the other micrograph shows the entire sorption of dye upon immersion of the entire photoconstruct [Fig. 10(B)].

Indomethacin was soaked in the entire body of microneedle-arrayed substrates from acetone solution. Upon implantation of microarchitectured implants with or without indomethacin loading into subcutaneous tissues of rats for 7 days, some histological differences between nonloaded and drug-loaded samples were observed. In the tissue facing the surface of nondrug-loaded photoconstruct some neutrophiles [stained by PAS reaction, Fig. 11(B)] and numerous newly recruited macrophage-like cells were present. A few giant foreign bodies, fused macrophages, were also seen [Fig. 11(A)]. On the contrary, such macrophage-like cells and neutrophiles were hardly seen in tissues facing the indomethacin-loaded surfaces [Fig. 11(C) and (D)]. This study indicates that the slow release of indomethacin from the microarchitectured surfaces appears to work well for modulation of foreign-body inflammatory reaction.

DISCUSSION

Stereolithography (SL) is a process of formulating three-dimensional (3D) plastic models from computer-aided manufacturing (CAM) technique using a combination of light beam, optical scannings, and photoreactive materials. This has been used for biomodeling to replicate the morphology of a biological structure in a solid substance.[17–19] The process uses a moving UV or visible light beam or laser beam, directed by a computer, to draw cross-sections of the model onto the surface of photocurable liquid polymer. In addition to biomodeling, microarchitectural surface design and entire-body design for advanced medical technology may be the next subject of SLA-based fabrication technology in biomedical applications.

To this end, we prepared photocurable liquid biodegradable copolymers that are photocured by UV or visible light irradiation. Because TMC units and CL units in copolymers are hydrolytically susceptible, these copolymers are essentially biodegraded. These hydrolyzed substances are essentially nontoxic. When TMG was used as an initiator, the resultant copolymer was hydrophobic and exhibited minimal water uptake, by which degradation proceeds preferentially via surface erosion upon immersion in aqueous alkaline solution as well as subcutaneous implantation. On the other hand, a PEG-based copolymer is hydrophilic and highly water sorpable, which induces the degradation both at the surface and in the bulk. Using these copolymers with different hydrolytic behaviors, a microarchitectural surface was designed by scanning photocurable liquid biodegradable copolymers films with a moving UV light beam. Stereolithographically microarchitectures were feasible as evidenced in the SEM micrographs. The thin liquid film of photocurable copolymers was easily photocured by UV irradiation. This enabled the layer-by-layer photocuring, as shown in Figure 3, resulting in a microphotoconstruct. Although SLA-driven photoconstructs have been utilized for shaping of automobiles and biomodeling of complex-shaped organs, few applications have utilized microfabrication of implant devices.

The CAD system enabled the automated preparation of microarchitectural surfaces as designed. Because the biodegradation rate can be manipulated by changing the mixture ratio of TMG-based and PEG-based vinylated copolymers or copolymer composition of TMC and CL, control of sustained release rate may be feasible. The SLA-driven microarchitecture may find versatile application in high precision-microfabricated biomedical devices.

The authors appreciate the histological examination by Dr. H. U. Ueda, Department of Pathology, National Cardiovascular Center Hospital (Osaka, Japan). One of the authors (M.M.) appreciates the continuous encouragement of Dr. G. N. Kumar, Dr. S. C. Arnold, and Dr. A. G. Scopelianos (all of whom are from Johnson & Johnson).

References

1. Mount GJ, Makinson OF, Peters MC. The strength of autocured and light-cured materials. The shear punch test. Aust Dent J 1996; 41:118.
2. Munoz J, Jimenez C, Bratov A, Bartroli J, Alegret S, Dominguez C. Photosensitive polyurethanes applied to the development of CHEMFET and ENFET devices for biomedical sensing. Biosens Bioelectron 1997;12:577.
3. Nishi S, Nakayama Y, Hashimoto N, Matsuda T. Basic fibroblast growth factor impregnated hydrogel microspheres for embolization of cerebral arteriovenous malformations. ASAIO J 1998;44:M405.
4. Vasiliskov AV, Timofeev EN, Surzhikov SA, Drobyshev AL, Shick VV, Mirzabekov AD. Fabrication of microarray of gel-immobilized compounds on a chip by copolymerization. Biotechniques 1999;27:592.
5. Matsuda T, Mizutani M, Arnold SC. Molecular design of photocurable liquid biodegradable copolymers. 1. Synthesis and photocuring characteristics. Macromolecules 2000;33:795.

6. Matsuda T, Mizutani M. Molecular design of photocurable liquid biodegradable copolymers. 2. Synthesis of coumarin-derivatized oligo(methacrylate)s and photocuring. Macromolecules 2000;33:791.
7. Matsuda T, Mizutani M. Photocurable liquid biodegradable copolymers: *In vitro* hydrolytic degradation behaviors of photocured films of coumarin-endcapped poly(ε-caprolactone-*co*-trimethylene carbonate). Biomacromolecules, to appear.
8. Matsuda T, Mizutani M. Liquid photocurable biodegradable copolymers: *In vivo* degradation of photocured poly(ε-caprolactone-*co*-trimethylene carbonate). J Biomed Mater Res. Forthcoming.
9. Matsuda T, Mizutani M, Arnold SC. Liquid, phenylazide-endcapped copolymers of ε-caprolactone and trimethylene carbonate: Preparation, photocuring characteristics and surface layering. Biomacromolecules. Forthcoming.
10. Mizutani M, Matsuda T. Liquid acrylate-endcapped biodegradable poly(ε-caprolactone-*co*-trimethylene carbonate). I. Preparation and visible-light-induced photocuring characteristics. J Biomed Mater Res 2002;62:387–394.
11. Albertsson A-C, Eklund M. Synthesis of copolymers of 1.3-dioxane-2-one and oxepan-2-one using coordination catalysts. J Polym Sci.Part A Polym Chem 1994;32:265.
12. Scopelianos AG, Bezwada RS, Arnold SC, Gooding RD. Liquid polymer filled envelopes for use as surgical implants. U.S. Pat. #5,411,554 (July, 1993).
13. Scopelianos AG, Arnold SC, Bezwada RS, Roller MB, Huxel ST. Injectable microdispersions for soft tissue repair and augmentation. U.S. Pat. #5,599852 (October, 1994).
14. Bezwada RS, Arnold SC, Shalaby WS. Liquid absorbable copolymers for parenteral application. U.S. Pat. #5,653,992 (April, 1995).
15. Scopelianos AG, Arnold SC, Bezwada RS, Roller MB, Huxel ST. Injectable microdipersions for soft tissue repair and augmentation. U.S. Pat. #5,728,752 (March, 1996).
16. Scopelianos AG, Bezwada RS, Arnold SC. Injectable liquid copolymers for soft tissue repair and augmentation. U.S. Pat. #5,824,333 (November, 1996).
17. Palser R, Jamieson R, Sutherland JB, Skibo L. Three-dimentional lithographic model building from volume data sets. Can Assoc Radiol J 1990; 41:339.
18. Poulsen M, Lindsay C, Sullivan T, D'Urso P. Stereolithographic modelling as an aid to orbital brachytherapy. Int J Radiat Oncol Biol Phys 1999;44:731.
19. Binder TM, Moertl D, Mundigler G, Rehak G, Franke M, Delle-Karth G, Mohl W, Baumgartner H, Maurer G. Stereolithographic biomodeling to create tangible hard copies of cardiac structures from echocardiographic data: In vitro and in vivo validation. J Am Coll Cardiol 2000;35:230.

Fabrication of micropored elastomeric film-covered stents and acute-phase performances

Yasuhide Nakayama,[1*] Shogo Nishi,[2*] Hatsue Ueda-Ishibashi,[3] Takehisa Matsuda[4]
[1]*Department of Bioengineering, National Cardiovascular Center Research Institute, 5-7-1 Fujishiro-dai, Suita, Osaka 565-8565, Japan*
[2]*Department of Neurosurgery, Takatsuki Sekijyuji Hospital, 1-1-1 Abuno, Takatuki, Osaka 569-1096, Japan*
[3]*Department of Pathology, National Cardiovascular Center Hospital, 5-7-1 Fujishiro-dai, Suita, Osaka 565-8565, Japan*
[4]*Department of Biomedical Engineering, Graduate School of Medicine, Kyushu University, 3-1-1 Maidashi, Higashi-ku, Fukuoka 812-8582, Japan*

Received 4 February 2002; accepted 27 February 2002

Abstract: To prevent thrombus formation in the acute phase and restenosis in the subacute to chronic phase after stenting of atherosclerotic arteries, we developed a covered stent with a micropored elastomeric film, the blood-contacting surface of which was coated with a photocured gelatin layer immobilized with heparin. Segmented polyurethane (SPU) film (30 μm in wall thickness) as a cover material was multiply micropored by excimer laser-directed microprocessing (pore diameter, 30 μm; interpore distance, 125 μm). An aqueous mixed solution of benzophenone-derivatized gelatin and heparin was coated on the micropored SPU film. Upon ultraviolet light irradiation, a thin layer of a gelatin gel immobilized with heparin was formed and simultaneously fixed on the SPU film. The fully covered stents were assembled by wrapping a balloon-expandable stent with gelatin/heparin gel-layered SPU film and subsequently suturing and then gluing. To assess the validity of this covered stent *in vivo*, "half-covered" stents, in which half at the distal side was covered with the gel-layered SPU film, was implanted in rabbit common carotid arteries (about 3 mm in diameter). After 3 months of implantation, all the half-covered stents ($n = 7$) were patent. Regardless of the covered or noncovered region of the stents, the entire luminal surface of the stents was fully endothelialized and a thin neointimal tissue was formed. The potential advantages of a covered stent as designed above are discussed. © 2002 Wiley Periodicals, Inc. J Biomed Mater Res 64A: 52–61, 2003

Key words: stent; cover; micropore; drug delivery; elastomeric polymer

INTRODUCTION

Percutaneous transluminal angioplasty in the coronary and peripheral arteries (PTCA or PTA) using either balloon catheters or metallic stents has been widely used for the clinical treatment of atherosclerotic stenosis.[1–6] Because of the reduced incidence of restenosis derived from excessive tissue ingrowth (intimal hyperplasia), endovascular metallic stenting has become more popular than balloon angioplasty (restenosis rate within 6 months after treatment: 25–30% for stent versus 30–50% for balloon). Many technical efforts aiming at a further-reduced restenosis rate have been made, especially in the structural design[7–10] of stents and biocompatible[7,11–13] and pharmacological coating[14–29] designs for struts of stents. In general, to minimize intimal hyperplasia, at least the following two factors should be incorporated into a stent design: 1. prevention of thrombus formation on the struts in the early implantation period, and 2. pharmacological effects minimizing tissue growth including cell proliferation and extracellular matrix production. The first one is particularly important because platelet-derived growth factor secreted from aggregated platelets in the thrombus is a potent mitogenic substance for smooth muscle cells (SMCs) which is one of the principal cells triggering intimal hyperplasia.[30,31] Previous articles have reported promising approaches via biocompatible designs including heparin derivatization and immobilization on struts,[23–27] thus minimizing thrombus formation, and pharmacological coatings[14–29] including sustained release of anti-cancer agents such as metalloproteinase inhibitor[15,16] and taxol,[21,22] thus

Correspondence to: T. Matsuda; e-mail: matsuda@med.kyushu-u.ac.jp
Contract grant sponsor: Promotion of Fundamental Studies in Health Science of the Organization for Pharmaceutical Safety and Research; contract grant number: 97-15
*Authors have contributed equally to this study.

reducing cell proliferation. The unexplored factor is 3. to construct or place a physical barrier[7-9] for the prevention or reduction of tissue ingrowth at the blood/stent interface.

Our attempts to reduce the restenosis rate of stents can be divided into two strategetic approaches: one approach is a photocured coating for struts,[19] which permits drug release and gene transfer. To this end, styrenated gelatin,[32,33] which was originally designed as a photocurable glue and a tissue-engineered scaffold, was mixed with model substances, such as protein and gene-encoding adenovirus, and photocured on struts by visible light-induced radical polymerization. Upon implantation in arteries, time-dependent permeation of a model protein and gene transfection from the stent-facing tissue to a deeper vascular tissue as well as a prolonged period of gene expression were noticed. Thus, photocurable gelatin served as a drug- or gene-delivery matrix.

The other approach under development is the loading of a physical barrier against tissue ingrowth on a stent, as mentioned above, which is also expected to serve as a pharmacological reservoir for drug or gene delivery. To this end, segmented polyurethane (SPU) elastomeric thin film with well-designed and fabricated micropores is wrapped to form a "covered" stent. This is based on our previous studies in which such a micropored SPU tube was photocured. Benzophenone-derivatized gelatin[34] mixed with heparin served as a small-diameter compliant graft[35,36] (wall thickness, 100 μm; inner diameter, 1.5 mm), and very high patency and rapid normal tissue regeneration without substantial intimal hyperplasia in arterial circulatory system were achieved. In this study, this heparin-loaded photocured gelatin-coated thin SPU film was used to cover a stent.

In contract, nonpermeable (or nonmicropored) artificial grafts provided very low patency. Our previous *in vivo* study[8] using a covered stent with regionally different pore densities showed that a higher pore density results in a lower degree of intimal hyperplasia under the particular condition of micrporosity densities examined. Based on these previous data, we developed a covered stent with a micropored elastomeric thin film and drug delivery function.

In this report, first we describe the fabrication method of the covered stent. Second, as a model device, we prepared "half-covered" stents in which half of each stent at the distal side was covered with the micropored film, and implanted them in the common carotid arteries of rabbits. This enabled us to demonstrate the validity of the concept of the covered stent with high reliability. That is, the effect of the covering on neointimal hyperplasia can be examined in a single animal using a single device by implantation of such a half-covered stent, thus minimizing the number of animal experiments and verifying our concept with high fidelity.

EXPERIMENTAL

Preparation of covered stents

SPU film (thickness, 30 μm; size, 15 × 7 mm; Sheedom Co., Tokyo, Japan) was used as the covering material, and microporing (diameter, 30 μm; interpore distance, 125 μm) of the film was performed using a KrF excimer laser microprocessing apparatus (model L4500; Hamamatsu Photonics, Hamamatsu, Japan).[37] One side of the micropored SPU film was coated with an aqueous solution (20 $\mu L/cm^2$) of benzophenone-derivatized gelatin[34] (benzophenone groups per gelatin molecule, 32 groups; 50 mg/mL) and heparin (25 mg/mL, 164.5 μ/mg; Wako Pure Chemical Ind., Osaka, Japan) and irradiated with a 400-W ultra-high-pressure mercury-vapor lamp (H-400-A/B; Irie Co., Tokyo, Japan). The treated surface of the film was placed on the outside of a balloon-expandable stent (Palmaz-Schatz; length, 15 mm; diameter, 1.2 mm; Johnson & Johnson Interventional Systems, Warren, NJ), and stay-sutured using 10-0 nylon thread under microscopy at six points. The film ends were overlapped, and adhered using a small amount of *N,N*-dimethylformamide (DMF) which is a good solvent for SPU, to prepare the covered stents.

Implantation

The experimental animals were seven New Zealand white rabbits, weighing 3–4 kg. The investigations were performed according to the Principles of Laboratory Animal Care (formulated by the National Society for Medical Research) and the Guide for the Care and Use of Laboratory Animals (National Institutes of Health Publication, No. 56-23, revised 1985). Heparin (2000 IU) was administered only during angiography. The covered stent mounted on a PTA balloon catheter (3.0 mm, 2 cm, SAVVY, Johnson & Johnson) was advanced into the common carotid artery (approximately 3 mm) from the femoral artery under fluoroscopy using a standard PTCA microguidewire. The balloon was inflated at a pressure of 8 atm for 30 s, deflated, and slowly withdrawn, leaving the covered stent in place. Neither antiplatelet agents nor additional anticoagulants were administerd during the 3-month follow-up period.

Microscopic examination

The implanted stents, including the surrounding common carotid artery tissues, were dissected free

and fixed with 10% formaldehyde in phosphate buffer (pH 7.4) for more than 48 h for light microscopy and scanning electron microscopy (SEM). Specimens for light microscopy were dehydrated with an alcohol series and embedded in glycolmethacrylate. Thin sections of the tissues were prepared in the direction of the circumference, subjected to standard hematoxylin and eosin staining, and observed under a light microscope (VANOX-S; OLYMPUS, Tokyo, Japan). Specimens for SEM were postfixed with 1% osmium tetraoxide, dehydrated in a graded series of ethanol, critical point dried, and sputter coated with platinum.

Morphometry

Using the National Institutes of Health Image software after calibration the thickness of the neointimal layer, defined as the distance between the endothelial lining and the stent strut or internal elastic lamina, was measured on top of and between the stent struts in at least three hematoxylin and eosin-stained sections at the proximal portion (bared region in the stent) and the distal portion (covered region) of each stented carotid segment.

Mechanical properties

The measurements of the tensile strength and the apparent elastic modulus of the SPU films were performed using a rheometer (RE-3305; Yamaden, Tokyo, Japan). The stress was recorded by continuous loading of strain to the films at a rate of 0.5 mm/s up to about 4 times extension. Apparent elastic modulus of the films were determined using the slope of the linear part of the strain–stress curve obtained at the initial extension.

RESULTS

Fabrication procedure

The fabrication procedure of the covered stent is shown in Figure 1, and the outline is described below. SPU film used as a covering film was subjected to laser ablation to create multiple micropores of a defined size (30 μm in diameter) and pore distribution (interpore distance, 125 μm) (step I in Fig. 1). Coating of a mixed aqueous solution of benzophenone-derivatized gelatin[34] and heparin and subsequent ultraviolet (UV) irradiation on one face of the micropored film produced a crosslinked gelatin layer which was immobilized with heparin (step II). A commercially available balloon-expandable stent was wrapped with the microporous SPU film with its treated surface facing inwards (step III). One end of the film was fixed to the stent strut by suturing (step IV). The other end was overlapped with the fixed end and adhered to it by gluing with DMF (step V). The detailed procedures for each step are described below.

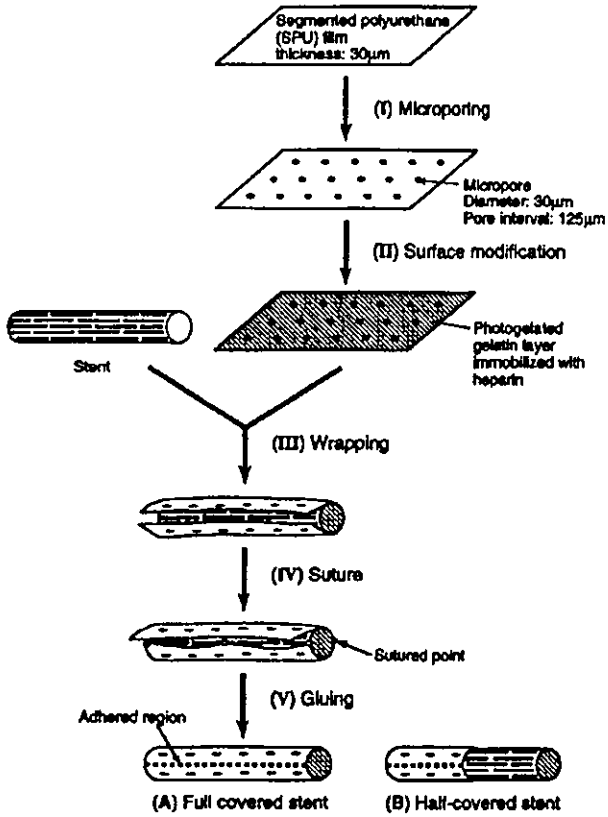

Figure 1. A schematic diagram of the preparation of the covered stent by microporing of SPU film with ablation by excimer laser (I), surface heparin immobilization using benzophenone-derivatized gelatin by UV irradiation (II), followed by covering the treated SPU film on a balloon-expandable stent (III, IV, V).

Microporing of the cover film (step I)

Microporing of the cover film was performed using a previously developed excimer laser ablation technique.[37] Irradiation of pulsed UV light from the excimer laser processing apparatus through a photomask with a round aperture 660 μm in diameter produced a micropattern of micropores 30 μm in diameter and with an interpore distance of 125 μm [Fig. 2(a, b)]. The mechanical properties of the micropored SPU films produced were examined by tensile strength tests. As shown in Figure 3, upon stretching the film, the strain of the film increased and concomi-

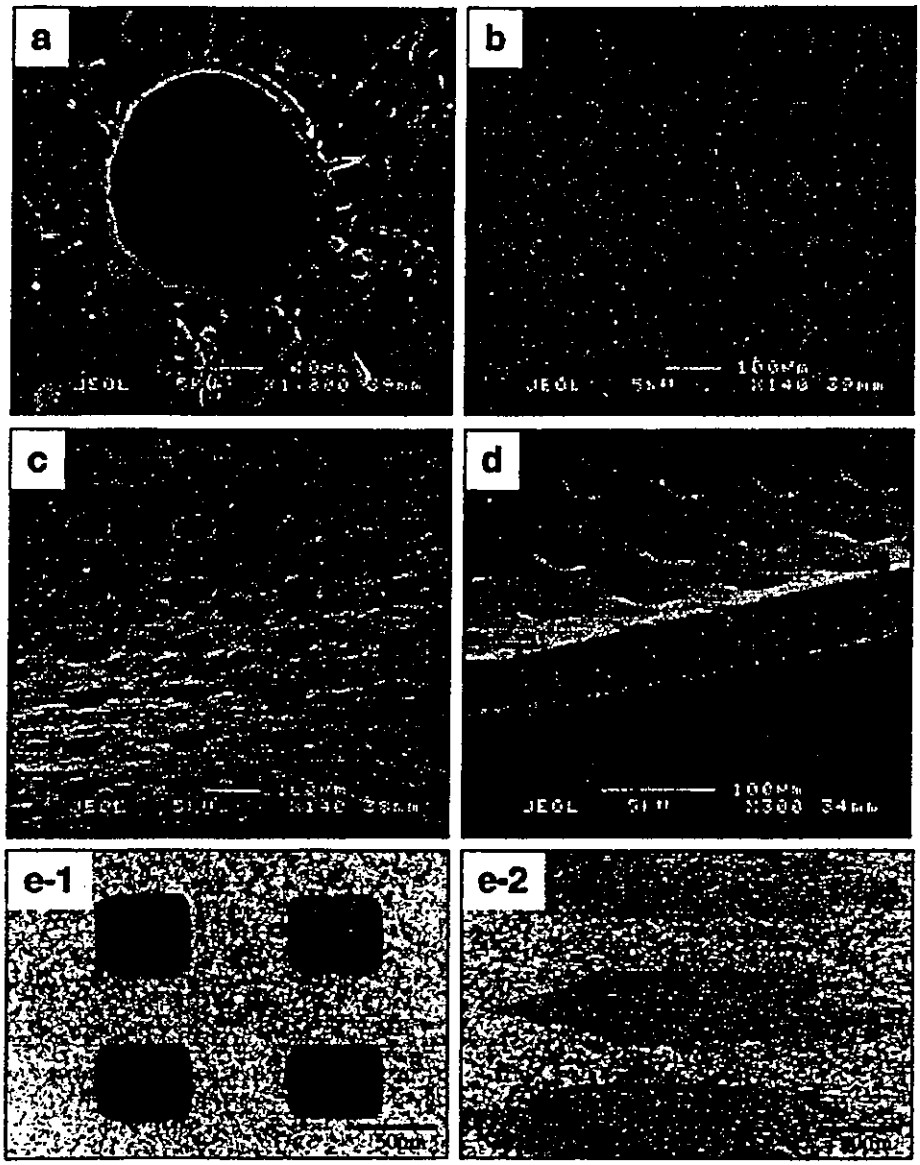

Figure 2. SEM of (a) the micropore and (b) multiple micropores, all of which were prepared by ablation with an excimer laser of SPU films, (c) multiply micropored SPU film after expanded upon about 4-times stretching from the original dimension in b, and (d) cross-section of the micropored SPU film surface-fixed with a heparin-immobilized gelatin layer, which was prepared by coating with the mixture of benzophenone-derivatized gelatin and heparin on the micropored SPU film and subsequent UV irradiation. Light micrographs of the SPU film partially surface-fixed with heparin-immobilized gelatin gel layer before (e-1) and after (e-2) stretching. The gelatin gel layer was fixed on only the dark-colored rectangular areas in e-1.

tantly the micropores were deformed from circles to ellipses [Fig. 2(c)]. The stress increased almost linearly within a range of strain up to 0.5, and the film was not ruptured by up to about 4 times of stretching from the original dimension. The elastic coefficient calculated was 1.60×10^7 Pa for the non-micropored film and 1.45×10^7 Pa for the micropored film.

Heparin immobilization on the cover film (step II)

One side of the microporous SPU film was coated with the aqueous solution of benzophenone-derivatized gelatin[34] and heparin, dried, and subsequently irradiated with UV light. The irradiated surface was slightly swollen in water, indicating the formation of a water-swellable gelatin gel layer. No delamination even upon vigorous rinsing with water was observed, indicating that the gelatin layer was tightly fixed to the SPU surface. SEM of the cross-section of the treated SPU film revealed that an approximately 5-μm-thick gelatin gel layer was formed on the coated surface, and the micropores were completely filled by the photocured gel [Fig. 2(d)]. To visualize heparin immobilized in the gel layer, the fol-

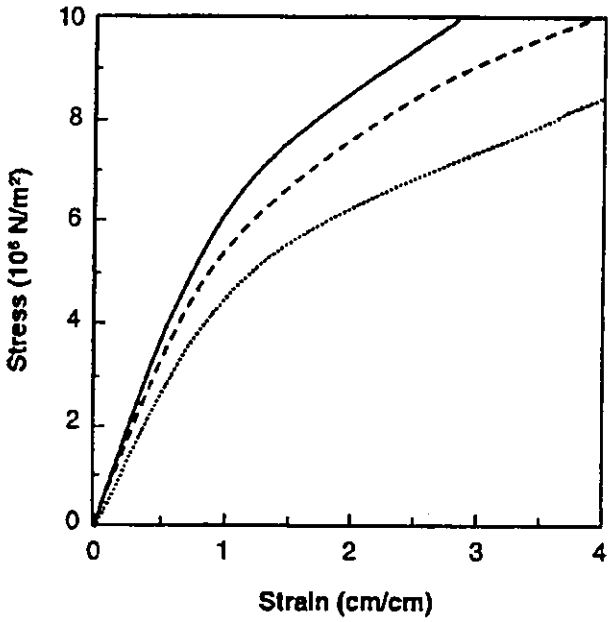

Figure 3. Stress–strain curves of nontreated SPU film (—), the micropored SPU films with an interpore distance of 125 μm (- - -), and the adhered SPU film (—). All films were expanded at a constant rate (0.5 mm/min) up to about 4-times stretching.

lowing experiment was separately conducted. The gelatin gel layer containing heparin was regionally prepared on SPU film by UV irradiation through a photomask with a lattice pattern, washed to remove non-photocured gelatin mixture, and immersed in an aqueous solution of a cationic dye, toluidine blue.[38] A blue–purple-stained lattice pattern was formed only at the gelatin-fixed area [Fig. 2(e-1)]. However, the film fixed with the gelatin without heparin was not stained by toluidine blue (data not shown). These results indicate that the formation of heparin-immobilized gel and fixation on SPU film simultaneously occurred by UV irradiation. When such a gelatin-fixed film was stretched, the gelatin layer was also synchronously stretched without delamination [Fig. 2 (e-2)].

Assembling of the covered stents (steps III, IV, V)

The heparin-immobilized gelatin gel layer-coated SPU film was placed so as to face the struts of stent, and one end of the film was wrapped and sutured to the struts at three sites using 10-0 nylon thread under microscopy. After the stent was tightly wrapped with the SPU film, the free ends of the film with a width of about 1 mm were overlapped, and adhered by gluing with DMF. The adhesion strength of the adhered SPU film was examined by tensile strength tests as described above. There was no rupture even when the film was expanded up to about 4 times stretching from the original dimension (Fig. 3). The elastic coefficient of the adhered film (1.2×10^7 Pa) was found to decrease to about two-thirds of that of the untreated micropored film. The covered stent was mounted on a PTA balloon catheter [Fig. 4(a)]. The covered stent was dilated by expanding a balloon with pressurized water [Fig. 4(b)]. After balloon deflation and subsequent removal of the balloon catheter, the shape of the stent was enough maintained without shrinkage [Fig. 4(c)]. As a model device for implantation, a half-covered stent was prepared by wrapping half of the outer surface of the stent strut with the heparin-loaded gelatin-layered SPU film similarly to the fully covered stent as mentioned above [Fig. 2(b)].

Implantation and histological evaluation

The half-covered stent, with the covered area on the distal side, was mounted in a PTA balloon-expandable

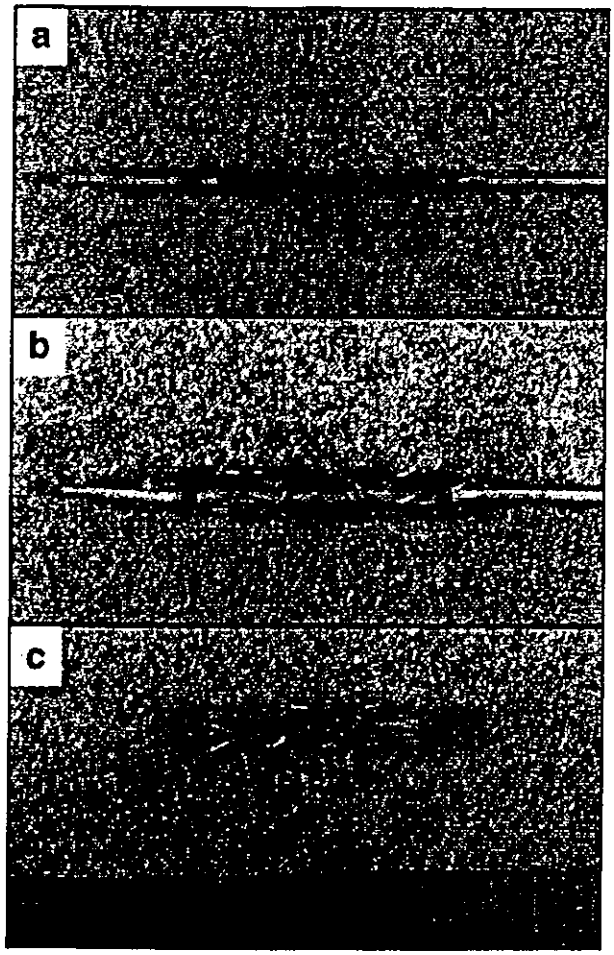

Figure 4. Gross appearance of the covered stent after mounting on a PTA balloon catheter (a), after dilation by expansion of the balloon (b), and after deflation and removal of the balloon (c).

catheter, and inserted from the femoral artery through a 5F sheath introducer, taking care not to slip both the stent and the cover film out of the balloon. The covered stents could be smoothly manipulated in blood vessels, and no differences in handling were noted irrespective of the presence of covering. The stent was navigated into the common carotid artery under fluoroscopy and placed by dilation of the PTA balloon. There was no difference in the dilation of the stent with or without covering.

Angiography immediately after implantation showed that all arteries (n = 7) were patent with no sign of intraluminal defects. In addition, angiography after 3-month implantation showed that all stents were patent. No significant intimal hyperplasia was macroscopically observed in the stent [Fig. 5(a)]. SEM observation indicated that the surface of the stent was covered with confluent endothelial cells in all cases, irrespective of covered or noncovered region (Fig. 6). The endothelial cells in all luminal surfaces exhibited a normal spindle shape and the direction of cellular elongation paralleled that of blood flow. This resembled the typical morphologic features of endothelial cells in natural vessels. Genesis of thin neointimal layers was observed around the strut in the noncovered stent region shown in the cross-section of the implanted sample [Fig. 5(b)]. In the covered region, thin neointimal layers were observed mainly on the surface of the film lumen, and the neogenetic and old intimal layers were united through the micropores produced on the film [Fig. 5(c)]. There was little difference in the neointimal layers between covered and noncovered regions. The mean thickness of the neointimal layers was 230.6 ± 57.5 μm in the uncovered region and 244.3 ± 48.5 μm including cover film thickness in the covered region.

DISCUSSION

For the treatment of arteriosclerotic stenosis lesions, stent angioplasty, which is much less invasive than the conventional surgical treatment, has widely been performed.[3–6] However, 25 – 30% of restenosis rates observed in a few months after stenting have been reported, which remains an unsolved problem. To reduce the restenosis rate as much as possible, various "second-generation" stents have been under development by incorporation of various working principles including surface designs such as polymer coating or fixation[19,39–46] and immobilization of pharmacological agents,[14–29] material designs such as metallic[47,48] for biocompatibility, and biodegradability and architectural design for flexibility and resistance against recoiling, as mentioned below.

The polymer materials used in these studies were degradable polymers such as polyglycolic acid[43] and polylactic acid[42–44] or nondegradable polymers such as polyurethane,[39,40] silicon,[46] and polyester.[41] However, it has been reported that stents covered with non-pored-polymer films implanted in the swine coronary artery caused significant inflammation, thrombus formation, and an excessive growth of SMCs, resulting in severe stenosis. This is because a covering film greatly increases the blood-contact surface area, which eventually increases the frequency of thrombus formation and inflammatory reaction. Therefore, a

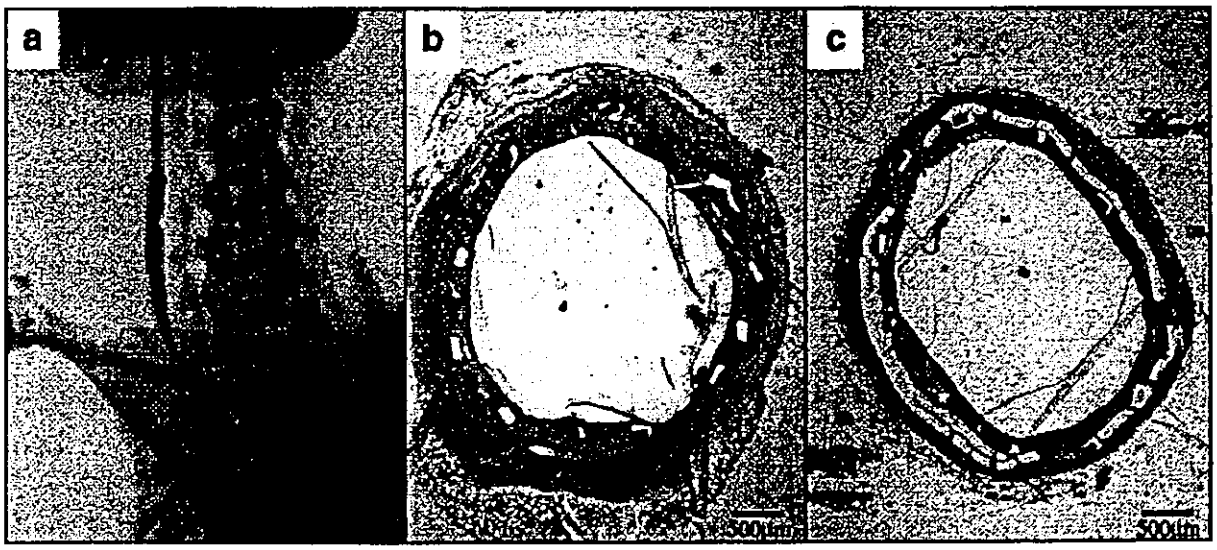

Figure 5. Angiograph of the rabbit common carotid artery after 3-month implantation of the half-covered stent (a). Light micrographs of the circumferential sections of the rabbit common carotid arteries implanted with the half-covered stent (c); bared region (b); and covered region (c) in the stent.

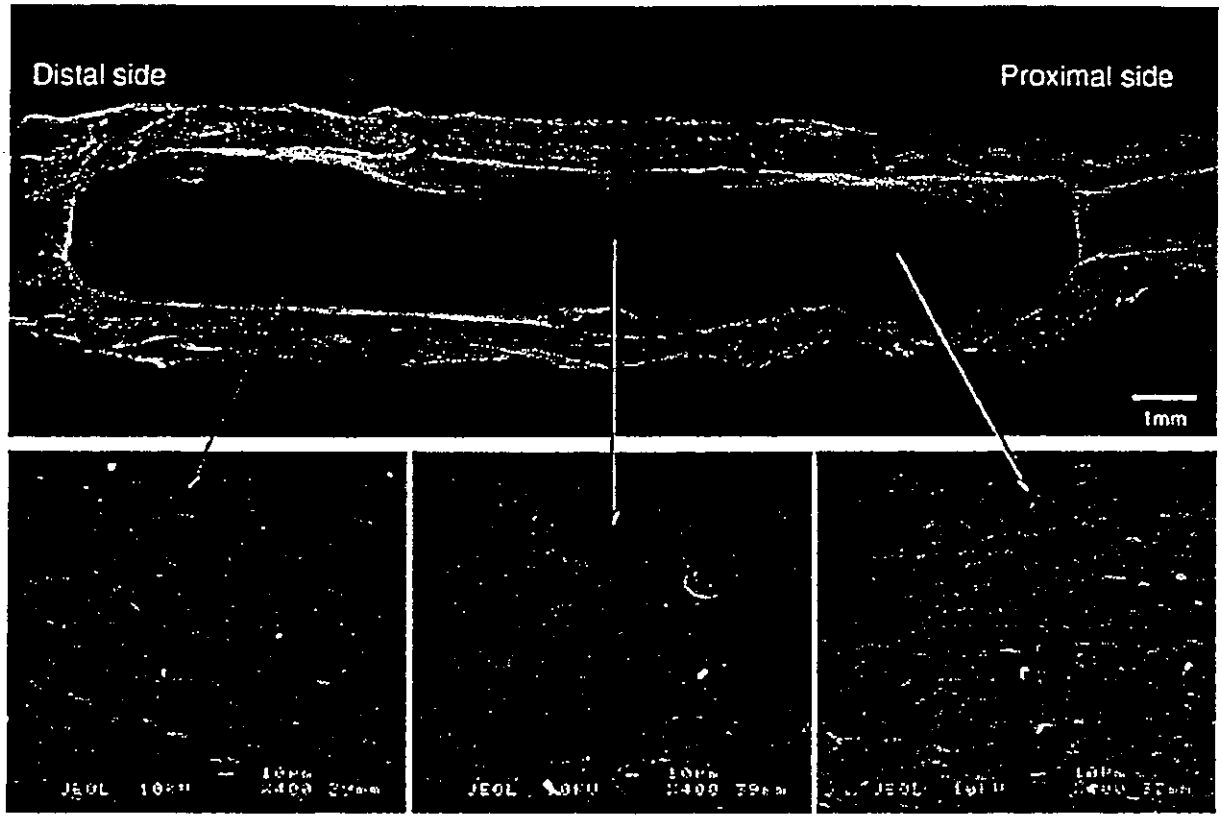

Figure 6. SEM of the luminal surface of the rabbit common carotid artery implanted with the half-covered stent.

high degree of anti-coagulation, minimal inflammation, and rapid endothelialization are essential properties for a "covered" stent. The first of these can be realized by heparin release from a gelatin gel-layered surface, the second may be achieved by using a nonbiodegradable biocompatible surface, and the last is mainly achieved by controlling the transmural tissue ingrowth of accompanying capillaries. Thus, microporosity is an essential factor for improved endothelialization and arterial tissue regeneration similar to the results observed for small-diameter artificial grafts[35,36] as well as a model "covered" stent in our previous study: SPU film-wrapped stents with regionally different pore densities in the circumferential configuration differentiated in the degree of tissue ingrowth, which depends on the pore density.[8]

In this study, we newly designed and devised a covered stent with the dual functions of drug reservoir/release and physical control of tissue ingrowth. Such a covering material should: 1. be a durable thin elastomeric film (which minimally increases the diameter of the stent because the diameter of diseased coronaries is approximately 3 mm, and that of stents in the nonexpanded state is approximately 1 ~ 1.5 mm but in the expanded state is approximately 3 mm). This means that approximately two- to three-fold stretching of the covered film occurred in the circumferential direction upon expansion; 2. be micropored with high-dimensional precision and at a well-defined pore density; and 3. provide a drug-loading matrix on both faces of the film surface. A drug-loaded covered film contacts with a much larger tissue area than a drug-loaded strut. SPU film was selected because it satisfies the requirements mentioned above in terms of durability, elasticity, high-quality microporing, and surface modification. Our previous article showed that precision processing of micropores at micron levels can be achieved using an ablation process with a pulsed excimer laser which has high energy in the UV region.[37,49] Multiple microporing, which is manipulated by computer-assisted design, reduced the elastic coefficient of the film (Fig. 3). The assembled covered stent could be easily expanded by inflation of an inserted balloon, in the same way as a noncovered stent. As the surface-layered drug-reservoir matrix, benzophenone-derivatized gelatin,[32] which was previously used for fabrication of SPU film-based small-diameter artificial grafts,[35,36] served effectively in stent application. Upon UV irradiation, radicals generated by photolysis of benzophenone groups lead to photocrosslinking between gelatin molecules as well as surface covalent bonding. Anti-coagulation was attained by impregnation of heparin in the photocured gelatin layer fixed on the SPU film. At 3-month implantation, all stents

were patent without significant intimal hyperplasia: there was little difference in the intimal thickness between the noncovered and covered regions of the "half-covered" stents, indicating that the immobilized and/or released heparin on the blood-contacting surface of the cover film effectively suppressed or minimized thrombus formation. Sooner or later, complete endothelialization on the struts of the stent and cover film appeared to proceed (Fig. 6). This was attributed to tissue ingrowth from both ends of the covered film as well as through the micropores [Fig. 5(b, c)], and indicates that, despite the presence of a foreign material, micropored SPU film did not significantly trigger the foreign body reactions that usually lead to excessive tissue ingrowth.

In this study, only the luminal surface (or blood-contacting face of film) was immobilized with heparin, simply focusing on anti-coagulation at the blood-contacting surface. However, drug loading on the tissue-facing surface may alter the morphogenesis process at athelosclerotic sites, reverting them to the normal tissue architecture if an appropriate drug is selected. Such candidate drugs may exert pharmacological or biological actions on cell proliferation, cell-cycle arrest, apoptosis, and/or phenotypic reversion of SMCs from "synthetic" to "contractile" type. That is, synthetic-phenotype SMCs, which exist in athelosclerotic sites, are highly proliferative and massively produce extracellular matrix components, both of which are major causes of intimal hyperplasia, whereas contractile-phenotype SMCs are in the quiescent state of their cell cycle—a phase of no-proliferation and no extracellular matrix synthesis, as is found in normal vascular tissue.[50,51]

In addition to suppressed intimal hyperplasia via sustained release from the matrix on the tissue-facing surface, the micropored film may act as a physical barrier controlling tissue ingrowth on the blood-contacting surface face in two manners. As shown in Figure 5c, vascular-type cells migrated from the tissue to the blood-contacting surface through micropores, resulting in neointimal tissue formation and subsequent endothelialization. Rapid endothelialization is the ultimate good for control of normal tissue regeneration. Our previous *in vitro*[49] and *in vivo*[8] studies revealed that optimal microporing is essentially needed for the control of cell migration from one side of the film surface to the other side, and that pore size and pore density are the real determinants for cellular migration and tissue ingrowth. As exemplified with other researchers' studies, nonpermeable films do not form neointimal tissue. Therefore, the high risk of continuous occurrence of thrombus is not circumvented in nature.

The other possible effect of a cover film on morphogenesis is to serve as a protective membrane resistant to "recoil" phenomena in the chronic phase,[52,53] in which SMCs which have accumulated in neointimal tissue and are highly elongated circumferentially self-contract to fasten the vessel wall: this generates inward tissue pressure, reducing the luminal diameter of a vessel. This recoiling often occurs after a prolonged period of implantation. The "protective or barrier membrane" may physically inhibit the "recoil" phenomena, whereas the minimally micropored area provides capillary-accompanying tissue ingrowth, resulting in endothelialization. Thus, by the concerted actions of sustained release of bioactive substances [for example, anti-coagulant (or heparin),[23–27] anti-proliferative agents (heparin for SMCs or anti-cancer agent[15,16,21,22] or cell-cycle modifier[28,29]), angiogenesis-inducing growth factor (or vascular endothelial growth factor)], and a physical barrier as mentioned above, intimal hyperplasia and mechanical recoiling may be prevented. This is our hypothetical appraisal of the "covered" stent and its potential performance in clinical situations.

To validate this hypothesis, we are now evaluating the usefulness of "full covered" stents using an animal model under conditions more directly resembling clinical applications: rabbits with hyperlipidemia and an intimal hypertrophy produced by balloon-induced denudation of endothelium are being used as an atherosclerotic animal model. The results for up to 7-month implantation will be reported in the near future.

References

1. Gruntzig AR, Senning A, Siegenthaler WE. Nonoperative dilation of coronary-artery stenosis: Percutaneous transluminal coronary angioplasty. N Engl J Med 1979;301:61–68.
2. Lee G, Ikeda RM, Joye JA, Bogren HG, DeMaria AN, Mason DT. Evaluation of transluminal angioplasty of chronic coronary artery stenosis: Value and limitations assessed in fresh human cadaver hearts. Circulation 1980;61:77–83.
3. Sigwart U, Puel J, Mirkovitch V, Joffre F, Kappenberger L. Intervascular stents to prevent occlusion and restenosis after transluminal angioplasty. N Engl J Med 1987;316:701–706.
4. Serruys PW, de Jaegere P, Kiemeneij F, Macaya C, Rutsch W, Heyndrickx G, Emanuelsson H, Marco J, Legrand V, Materne P, Belardi J, Sigwart U, Colombo A, Goy JJ, van der Heuvel P, Delcan J, Morel MA. A comparison of balloon-expandable-stent implantation with balloon angioplasty in patients with coronary artery disease. N Engl J Med 1994;331:489–495.
5. Fiscman DL, Leon MB, Baim DS, Schatz RA, Savage MP, Penn I, Detre K, Veltri L, Ricci D, Nobuyoshi M, Cleman M, Heuser R, Almond D, Teirstein PS, Fish RD, Colombo A, Brinker J, Moses J, Shaknovich A, Hirshfeld J, Bailey S, Ellis S, Rake R, Goldberg S. A randomized comparison of coronary-stent placement and balloon angioplasty in the treatment of coronary artery disease. N Engl J Med 1994;331:496–501.
6. Erbel R, Haude M, Hopp HW, Franzen D, Rupprecht HJ, Heublein B, Fisher K, de Jaegere P, Serruys P, Rutsch W, Probst P. Coronary-artery stenting compared with balloon angioplasty for restenosis after intimal balloon angioplasty. N Engl J Med 1998;339:1672–1678.

7. Van der Giessen WJ, Lincoff AM, Schwartz RS, van Beusekom HM, Serruys PW, Holmes DR Jr, Ellis SG, Topol EJ. Marked inflammatory sequelae to implantation of biodegradable and nonbiodegradable polymers in porcine coronary arteries. Circulation 1996;94:1690–1697.
8. Nakayama Y, Nishi S, Ishibashi-Ueda H, Matsuda T. Surface microarchitectural design in biomedical applications: *In vivo* analysis of tissue ingrowth in excimer laser-directed micropored scaffold for cardiovascular tissue engineering. J Biomed Mater Res 2000;51:520–528.
9. Uematsu M, Okada M. Self-expandable vascular stent covered with polyurethane membrane: An experimental preliminary study of a placement in the thoracic descending aorta of a rabbit using endovascular intervention. Ann Thorac Cardiovasc Surg 2000;6:137–141.
10. McKenna CJ, Camrud AR, Sangiorgi G, Kwon HM, Edwards WD, Holmes DR Jr, Schwartz RS. Fibrin-film stenting in a porcine coronary injury model: Efficacy and safety compared with uncoated stents. J Am Coll Cardiol 1998;31:1434–1438.
11. De Scheerder I, Szilard M, Yanming H, Ping XB, Verbeken E, Neerinck D, Demeyere E, Coppens W, Van de Werf F. Evaluation of the biocompatibility of two new diamond-like stent coatings (Dylyn) in a porcine coronary stent model. J Invasive Cardiol 2000;12:389–394.
12. Whelan DM, van der Giessen WJ, Krabbendam SC, van Vliet EA, Verdouw PD, Serruys PW, van Beusekom HM. Biocompatibility of phosphorylcholine coated stents in normal porcine coronary arteries. Heart 2000;83:338–345.
13. Bertrand OF, Sipehia R, Mongrain R, Rodes J, Tardif JC, Bilodeau L, Cote G, Bourassa MG. Biocompatibility aspects of new stent technology. J Am Coll Cardiol 1998;32:562–571.
14. Lahann J, Klee D, Pluester W, Hoecker H. Bioactive immobilization of γ-hirudin on CVD-coated metallic implant devices. Biomaterials 2001;22:817–826.
15. de Smet BJ, de Kleijn D, Hanemaaijer R, Verheijen JH, Robertus L, van Der Helm YJ, Borst C, Post MJ. Metalloproteinase inhibition reduces constrictive arterial remodeling after balloon angioplasty: A study in the atherosclerotic Yucatan micropig. Circulation 2000;101:2962–2967.
16. Cherr GS, Motew SJ, Travis JA, Fingerle J, Fisher L, Brandl M, Williams JK, Geary RL. Metalloproteinase inhibition and the response to angioplasty and stenting in atherosclerotic primates. Arterioscler Thromb Vasc Biol 2002;22:161–166.
17. Lincoff AM, Furst JG, Ellis SG, Tuch RJ, Topol EJ. Sustained local delivery of dexamethasone by a novel intravascular eluting stent to prevent restenosis in the porcine coronary injury model. J Am Coll Cardiol 1997;29:808–816.
18. Yamawaki T, Shimokawa H, Kozai T, Miyata K, Higo T, Tanaka E, Egashira K, Shiraishi T, Tamai H, Igaki K, Takrshita A. Intramural delivery of a specific tyrosine kinase inhibitor with biodegradable stent suppresses the restenotic changes of the coronary artery in pigs *in vivo*. J Am Coll Cardiol 1998;32:780–786.
19. Nakayama Y, Ji-Youn K, Nishi S, Ueno H, Matsuda T. Development of high-performance stent: Gelatinous photogel-coated stent that permits drug delivery and gene transfer. J Biomed Mater Res 2001;57:559–566.
20. Lambert TL, Dev V, Rechavia E, Forrester JS, Litvack F, Eigler NL. Localized arterial wall drug delivery from a polymer-coated removable metallic stent: Kinetics, distribution, and bioactivity of forskolin. Circulation 1994;90:1003–1011.
21. Farb A, Heller PF, Shroff S, Cheng L, Kolodgie FD, Carter AJ, Scott DS, Froehlich J, Virmani R. Pathological analysis of local delivery of paclitaxel via a polymer-coated stent. Circulation 2001;104:473–479.
22. Heldman AW, Cheng L, Jenkins GM, Heller PF, Kim DW, Ware M Jr, Nater C, Hruban RH, Rezai B, Abella BS, Bunge KE, Kinsella JL, Sollott SJ, Lakatta EG, Brinker JA, Hunter WL, Froehlich JP. Paclitaxel stent coating inhibits neointimal hyperplasia at 4 weeks in a porcine model of coronary restenosis. Circulation 2001;103:2289–2295.
23. Hardhammar PA, van Beusekom HMM, Emanuelsson HU, Hofma SH, Albertsson PA, Verdouw PD, Boersma E, Serruys PW, van der Giessen WJ. Reduction in thrombotic events with heparin-coated Palmaz-Schatz stents in normal porcine coronary arteries. Circulation 1996;93:423–430.
24. Blezer R, Cahalan L, Cahalan PT, Lindhout T. Heparin coating of tantalum coronary stents reduces surface thrombin generation but not factor IXa generation. Blood Coagul Fibrinolysis 1998;9:435–440.
25. van Der Giessen WJ, van Beusekom HM, Larsson R, Serruys P. Heparin-coated coronary stents. Curr Interv Cardiol Rep 1999; 1:234–240.
26. Beythien C, Gutensohn K, Bau J, Hamm CW, Kuhnl P, Meinertz T, Terres W. Influence of stent length and heparin coating on platelet activation: A flow cytometric analysis in a pulsed floating model. Thromb Res 1999;94:79–86.
27. Vrolix MC, Legrand VM, Reiber JH, Grollier G, Schalij MJ, Brunel P, Martinez-Elbal L, Gomez-Recio M, Bar FW, Bertrand ME, Colombo A, Brachman J. Heparin-coated Wiktor stents in human coronary arteries (MENTOR trial). MENTOR Trial Investigators. Am J Cardiol 2000;86:385–389.
28. Sousa JE, Costa MA, Abizaid AC, Rensing BJ, Abizaid AS, Tanajura LF, Kozuma K, Van Langenhove G, Sousa AG, Falotico R, Jaeger J, Popma JJ, Serruys PW. Sustained suppression of neointimal proliferation by sirolimus-eluting stents: One-year angiographic and intravascular ultrasound follow-up. Circulation 2001;104:2007–2011.
29. Sousa JE, Costa MA, Abizaid A, Abizaid AS, Peres F, Pinto IM, Seixas AC, Staico R, Mattos LA, Sousa AG, Falotico R, Jaeger J, Popma JJ, Serruys PW. Lack of neointimal proliferation after implantation of Sirolimus-coated stents in human coronary arteries: A quantitative coronary angiography and three-dimensional intravascular ultrasound study. Circulation 2001; 103:192–195.
30. Jawien A, Bowen-Pope DF, Libdner V, Schwartz SM, Clowes AW. Platelet-derived growth factor promotes smooth muscle migration and intimal thickening in a rat model of balloon angioplasty. J Clin Invest 1992;89:507–511.
31. Pitsch RJ, Minion DJ, Goman ML, van Aalst JA, Fox PL, Graham LM. Platelet-derived growth factor production by cells from Dacron grafts implanted in a canine model. J Vasc Surg 1997;26:70–78.
32. Nakayama Y, Okuda K, Matsuda T. Preparation of multifunctional gelatin or albumin-based macromors and visible light-induced gelation of these aqueous solutions. Biomacromolecules. Submitted for publication.
33. Okino H, Nakayama Y, Tanaka M, Matsuda T. *In situ* hydrogelation of photocurable gelatin and drug release. J Biomed Mater Res 2002;59:233–245.
34. Nakayama Y, Matsuda T. Photocurable surgical tissue adhesive glues composed of photorective gelatin and poly(ethylene glycol) diacrylate. J Biomed Mater Res 1999;48:511–521.
35. Doi K, Nakayama Y, Matsuda T. Novel compliant and tissue-permeable microporous polyurethane vascular prosthesis fabricated using an excimer laser ablation technique. J Biomed Mater Res 1996;31:27–33.
36. Doi K, Matsuda T. Significance of porosity and compliance of microporous, polyurethane-based microarterial vessel on neoarterial wall regeneration. J Biomed Mater Res 1997;37:573–584.
37. Nakayama Y, Matsuda T. Surface microarchitectural design in biomedical applications: Preparation of microporous polymer surfaces by an excimer laser ablation technique. J Biomed Mater Res 1995;29:1295–1301.
38. Smith PK, Mallia AK, Mermanson GT. Colorimetric method

for the assay of heparin content in immobilized heparin preparations. Anal Biochem 1980;109:466–473.
39. Holmes DR, Camrud AR, Jorgenson MA, Edwards WD, Schwartz RS. Polymeric stenting in the porcine coronary artery model: Differential outcome of exogenous fibrin sleeves versus polyurethane-coated stents. J Am Coll Cardiol 1994;24:525–531.
40. Severini A, Mantero S, Tanzi MC, Cigada A, Salvetti M, Cozzi G, Motta A. Polyurethane-coated, self-expandable biliary stent: An experimental study. Acad Radiol 1995;2:1078–1081.
41. Castaneda F, Ball SM, Wyffels PL, Young K, Li R. Assessment of a polyester-covered nitinol stent in an atherosclerotic swine model. J Vasc Interv Radiol 2000;11:483–491.
42. Schellhammer F, Berlis A, Bloss H, Pagenstecher A, Schumacher M. Poly-lactic-acid coating for endovascular stents: Preliminary results in canine experimental arteriovenous fistulae. Invest Radiol 1997;32:180–186.
43. Hietala EM, Salminen US, Stahls A, Valimaa T, Maasilta P, Tormala P, Nieminen MS, Harjula AL. Biodegradation of the copolymeric polylactide stent: Long-term follow-up in a rabbit aorta model. J Vasc Res 2001;38:361–369.
44. Tamai H, Igaki K, Kyo E, Kosuga K, Kawashima A, Matsui S, Komori H, Tsuji T, Motohara S, Uehata H. Initial and 6-month results of biodegradable poly-L-lactic acid coronary stents in humans. Circulation 2000;102:399–404.
45. Petas A, Vuopio-Varkila J, Siitonen A, Valimaa T, Talja M, Taari K. Bacterial adherence to self-reinforced polyglycolic acid and self-reinforced polylactic acid 96 urological spiral stents *in vitro*. Biomaterials 1998;19:677–681.
46. Ozbek C, Heisel A, Gross B, Bay W, Schieffer H. Coronary implantation of silicone-carbide-coated Palmaz-Schatz stents in patients with high risk of stent thrombosis without oral anticoagulation. Cathet Cardiovasc Diagn 1997;41:71–78.
47. Kastrati A, Schomig A, Dirschinger J, Mehilli J, von Welser N, Pache J, Schuhlen H, Schilling T, Schmitt C, Neumann FJ. Increased risk of restenosis after placement of gold-coated stents: Results of a randomized trial comparing gold-coated with uncoated steel stents in patients with coronary artery disease. Circulation 2000;30:2478–2483.
48. Edelman ER, Seifert P, Groothuis A, Morss A, Bornstein D, Rogers C. Gold-coated NIR stents in porcine coronary arteries. Circulation 2001;103:429–434.
49. Matsuda T, Nakayama Y. Surface microarchitectural design in biomedical applications: *In vitro* transmural endothelialization on microporous segmented polyurethane films fabricated using an excimer laser. J Biomed Mater Res 1996;31:243–249.
50. Neuville P, Yan Z, Gidlof A, Pepper MS, Hansson GK, Gabbiani G, Sirsjo A. Retinoic acid regulates arterial smooth muscle cell proliferation and phenotypic features *in vivo* and *in vitro* through an RARalpha-dependent signaling pathway. Arterioscler Thromb Vasc Biol 1999;19:1430–1436.
51. Kocher O, Gabbiani F, Gabbiani G, Reidy MA, Cokay MS, Peters H, Huttner I. Phenotypic features of smooth muscle cells during the evolution of experimental carotid artery intimal thickening: Biochemical and morphologic studies. Lab Invest 1991;65:459–470.
52. Chan AW, Moliterno DJ. In-stent restenosis: Update on intracoronary radiotherapy. Cleve Clin J Med 2001;68:796–803.
53. Mintz GS. Remodeling and restenosis: Observations from serial intravascular ultrasound studies. Curr Interv Cardiol Rep 2000;2:316–325.

TISSUE ENGINEERING
Volume 9, Number 1, 2003

Human Endothelial Progenitor Cell-Seeded Hybrid Graft: Proliferative and Antithrombogenic Potentials *in Vitro* and Fabrication Processing

TOSHIHIKO SHIROTA, M.D.,[1,2] HONGBING HE, M.D.,[3] HISATAKA YASUI, M.D., Ph.D.,[2] and TAKEHISA MATSUDA, Ph.D.[1]

ABSTRACT

In this article, we show that human endothelial progenitor cells (EPCs) in circulating peripheral blood may be a novel cell source for a cell-incorporated engineered vascular graft. Cultures of human peripheral blood mononuclear cells collected by the density gradient technique developed highly proliferative EPC colonies, which expanded with culture time. The production rates of antiplatelet substances such as endothelial-type nitric oxide synthase and 6-keto-prostaglandin-F_1-α were approximately one-third and approximately one-half of those of mature endothelial cells (ECs), respectively. On the other hand, the tissue-type plasminogen activator production rate of EPCs was almost the same as that of ECs. EPCs were seeded and cultured on a small-diameter compliant graft (inner diameter, 1.5 mm) made of microporous segmented polyurethane film coated with a photoreactive gelatin layer, and subsequently subjected to hydrodynamic shear stress by *ex vivo* circulation. EPCs fully covering the graft elongated and aligned themselves with the direction of the flow, resulting in the production of an integrated EPC-engineered graft. These results indicate that EPCs, which have high proliferative potential and high antithrombogenic potential, comparable to those of ECs, are a suitable cell source for cardiovascular tissue engineering.

INTRODUCTION

AN ENDOTHELIAL CELL (EC) MONOLAYER formed on the lumenal surface of a synthetic graft has been proved to be antithrombogenic because of its inherent antithrombogenic potential to express potent antiplatelet, anticoagulant, and high fibrinolytic activities. In the past 20 years,[1] many experimental studies have been reported on the EC-seeded small-diameter vascular graft with high patency derived from improved seeding techniques and optimally designed extracellular matrix layering methods. Clinical studies indicate that the EC-seeded graft has high patency rates in human cardiac artery bypass grafting[2] and in lower extremity artery bypass grafting.[3] Despite such successful results, however, the clinical application of the EC-seeded graft is still hampered by the lack of a convenient source of ECs.

A few articles have reported the existence of endothelial progenitor cells (EPCs) in human adult peripheral blood, and the contribution of these cells to adult vasculogenesis.[4–7] These studies suggest that it is possible to isolate and expand EPCs obtained from peripheral blood for cell-seeded vascular prostheses. The advantage of using EPCs as a new source for vascular tissue engineering is that the procedure is much less invasive than the surgical harvest of ECs from large veins or tissue microvessels of

[1]Department of Biomedical Engineering, Graduate School of Medicine, Kyushu University, Fukuoka, Japan.
[2]Department of Cardiac Surgery, Graduate School of Medicine, Kyushu University, Fukuoka, Japan.
[3]Department of Biomedical Engineering, National Cardiovascular Center Research Institute, Osaka, Japan.